The effect of the MJO on the North American Monsoon

David J. Lorenz and Dennis L. Hartmann

Department of Atmospheric Science,

University of Washington

Submitted to J. Climate

Corresponding Author: David J. Lorenz, djlorenz@atmos.washington.edu

July 9, 2004

Abstract

The effect of the MJO in the eastern Pacific on the North American monsoon is documented using NCEP Reanalysis and daily-mean precipitation data from 1958-2003. It is found that westerly zonal wind anomalies in the eastern tropical Pacific lead to above normal precipitation in northwest Mexico and Arizona several days to over a week later. This connection between the tropical Pacific and monsoon precipitation appears to be limited to regions influenced by moisture surges from the Gulf of California as a similar connection does not exist for New Mexico precipitation. The evidence suggests that the MJO affects monsoon precipitation by modulating the strength of easterly waves off the coast of Mexico, which in turn trigger the development of a gulf surge.

1. Introduction

The North American Monsoon (NAM) is a climate phenomenon in the southwest United States and northwest Mexico that typically begins in early July and lasts until September. It is associated with a dramatic increase in precipitation over what is normally an arid region of North America (Douglas et al. 1993; Adams and Comrie 1997).

In this study, we want to better understand processes which control intraseasonal variability of monsoon precipitation. In particular, we will focus on the role of the Madden-Julian Oscillation (MJO, see Madden and Julian 1971, 1994) in modulating precipitation in the NAM. Previous studies on the effect of MJO on North American summer precipitation have emphasized the strong MJO signal in southern Mexico (Higgins and Shi 2001). In this study, we want to focus on the effect of the MJO on precipitation in the monsoon region of Arizona, New Mexico and northwest Mexico.

In section 2, we describe the data and the basic analysis methods. In section 3, we begin by demonstrating the connection between the MJO and monsoon precipitation, and continue by describing in more detail the time evolution of the wind and precipitation anomalies associated with this connection. We also provide a dynamical mechanism to explain the observed effect of the MJO on monsoon precipitation. We end with the conclusions in section 4.

2. Data and Analysis

The wind and geopotential height data come from the NCEP Reanalysis (Kalnay et al. 1996) on a 2.5° × 2.5° latitude/longitude grid. The 24-hour-mean precipitation data come from US and Mexico station data interpolated to a 1° × 1° latitude/longitude grid using a Modified Cressman (1959) Scheme (Glahn et al. 1985; Charba et al. 1992). The

precipitation data set is available from the Climate Prediction Center (CPC) from their website: http://www.cpc.ncep.noaa.gov/products/precip/realtime/retro.html. The US portion of the analysis was based on the CPC Unified Precipitation Data Set (Higgins et al. 2000) and the Mexico portion was based on daily station data from about 300 gauge stations prior to the 1990's and about 600 gauge stations afterwards. We use daily NCEP reanalysis data at 12UTC which is early morning local time at the start of the 24-hour-mean precipitation data.

We use data from 1958 to 2003 during the North American Monsoon season (late June to early September). For some of our results, we average the daily data in time into 3-day-mean (triad), 5-day-mean (pentad) and weekly-mean data. The precise season varies with the amount of time averaging such that the season length is a multiple of 3, 5 or 7 (see Table 1). We use a variety of time averaging in order to best present the results of this study: daily and triad data give the best time resolution in order to clearly show evolution of events in time, while pentad and weekly data improve signal to noise ratio. The basic results and conclusions of this study are evident regardless of the amount of time averaging.

We find anomaly data by removing the mean seasonal cycle which is a smoothed version of the 46 year climatology. The climatology is smoothed with a 1-2-1 time filter. The 1-2-1 filter is applied once for the weekly and pentad data and is applied five times for the triad and daily data. The results are not sensitive to the amount of smoothing. After we remove the annual cycle we subtract the seasonal-mean anomaly from the data in order to remove the interannual variability.

For most of the results, we use linear regression analysis rather than compositing analysis. The same general patterns and conclusions result for both techniques. We choose to use regression analysis because the results are smoother and the technique is more objective. For the time-lagged regression analysis, we use data outside of the seasons specified in Table 1. For example, when regressing the wind on a time series with a time lag of 3 days, we use wind data from September 4 even though the season technically ends on September 1.

Statistical significance is determined using a two-sided t-test with a significance level of 95%.

3. Results

a) Definition of precipitation indices

To study effect of MJO on the monsoon we form precipitation indices which are the average precipitation over a localized region at a given time. The three representative regions which summarize the connection between the MJO and the North American Monsoon (NAM) are called the southern Arizona region (S AZ), the southwest New Mexico region (SW NM) and the northwest Mexico region (NW Mex.) (Fig. 1). The correlation between the indices for weekly-mean data is also shown in figure 1. The precise boundaries of the three regions are given in Table 2. Note that the correlations between adjacent regions are quite small even for weekly mean data.

The lag-correlation summarizes the relationship between the precipitation regions in time (Fig. 2). The lag-correlation between the S AZ and SW NM indices implies that precipitation in these regions tends to occur on the same day, although the correlation drops off less rapidly in time when S AZ leads SW NM. Figure 2b is clearly much

different than 2a and indicates that precipitation in NW Mex. tends to lead S AZ by about two days. This time lag might be a signature of moisture surges from the Gulf of California which tend to reach NW Mex. before S AZ. A similar but not as pronounced time lag is also evident between NW Mex. and SW NM.

b) Connection to tropics

To investigate the relationship between NAM precipitation and the large-scale circulation we regress the 850mb zonal wind on the three precipitation indices defined above (Fig. 3). Note that the precipitation indices lag the zonal wind so that Figure 3 shows the wind anomalies which precede the rain events. In this study, we will emphasize the wind anomalies in the tropics which are a signature of the MJO.

Looking at Figure 3, we see that statistically significant zonal wind anomalies in the East Pacific at 12.5°N precede precipitation in S AZ and NW Mex. but not in SW NM. As shown in previous studies (Maloney and Hartmann 1998, 2001), the 850mb zonal wind in this region is directly related to the MJO. We provide further evidence suggesting that this East Pacific wind variability is directly related to the MJO by forming an index of 850mb zonal wind in this region. Our index is the average zonal wind anomalies over the box in the East Pacific (see Fig. 3d). We also form a second index in the West Pacific (see box in Fig. 3d) where negative anomalies are evident in Figure 3ac. The power spectra over the entire warm season (May-Sept.) show a statistically significant peek at a period of about 50 days for both the East and West Pacific indices (Fig. 4a). Moreover, the coherence squared becomes quite large at periods of 38 and 50 days demonstrating that the variability in these two widely separated regions reflects the dynamics of a global-scale mode (Fig. 4b). The preferred period and global-scale nature

of the variability in the tropical Pacific implies that the variability is directly related to the MJO. The fact that Monsoon precipitation is most correlated with the East Pacific portion of the global anomalies suggests that the global-scale MJO and the NAM region are linked through processes in the East Pacific.

As an aside, we note that although the MJO signal preceding NAM precipitation is significant for S AZ but not for SW NM, both S AZ and SW NM share a similar extra-tropical north/south zonal wind dipole in the North Pacific (Fig. 3ab).

The reasons for the MJO link to S AZ precipitation but not SW NM precipitation become clearer when we look at the 850mb winds and heights at the time of the precipitation events (Fig. 5). Rainfall in S AZ is typically associated with a strong surge of southerly wind from the Gulf of California, while rainfall in SW NM is usually associated with easterly, upslope winds from the Great Plains. Thus, it appears that the MJO influences NAM rainfall through its effect on surges of moisture from the Gulf of California ("gulf surges"). Because most of SW NM lies on the eastern side of the continental divide the affect of gulf surges on NM rainfall is much less than AZ. We will explore the mechanism connecting the MJO and gulf surges below, but first we will look at the time evolution of the East Pacific zonal wind and NAM precipitation in more detail.

c) Time Evolution

We summarize the time evolution of the tropical zonal wind associated with NAM precipitation by regressing the zonal wind along 12.5°N with the precipitation indices for different time lags (Fig. 6). As seen previously in figure 3, statistically significant zonal wind anomalies in the East Pacific precede NAM precipitation. In

addition to this feature, figure 6 also shows that negative wind anomalies follow the precipitation events. These negative anomalies exist because the MJO is a quasi-periodic phenomenon so that negative anomalies tend to follow positive anomalies. Also note the somewhat out of phase anomalies in the West Pacific which accompany the East Pacific anomalies. Although these anomalies barely pass the significance level for the S AZ case, we believe these anomalies indicate a real, physical connection because nearly out-of-phase West Pacific anomalies accompany MJO anomalies in the East Pacific (e.g. Maloney and Hartmann 1998). Also note that the wind anomalies associated with NW Mex. are shifted in time by roughly one triad (3-day-mean data) compared to S AZ which is consistent with the idea that the MJO affects the monsoon through gulf surges–the gulf surges reach NW Mex. before S AZ. The 12.5°N zonal wind plot for SW NM precipitation has weak statistically insignificant anomalies (not shown).

To show the time evolution of the precipitation associated with East Pacific wind anomalies, we correlate the East Pacific zonal wind index defined previously (see Fig. 3d) with the precipitation anomalies for different time lags (Fig. 7). At the time of maximum zonal wind anomalies (lag = 0), the precipitation is strongest along the Pacific coast in southern Mexico (see also Higgins and Shi 2001). These precipitation anomalies extend northward to the southern edge of the NAM region. Also note that statistically significant anomalies extend northward into southern Texas at this time. In the U.S. portion of the NAM region, however, the precipitation anomalies are basically zero or perhaps even negative. Three days later (lag = 1 triad) the anomalies extend up to the international border and by nine days later (lag = 3 triads) the anomalies in southern and central Arizona are among the strongest on the map. An important result evident in figure

7 is that the MJO related precipitation anomalies do *not* extend into New Mexico yet southwest New Mexico clearly experiences the monsoon-type climate (e.g. Douglas et al. 1993). If the MJO affects the NAM through gulf surges, then this result is consistent with the idea that *both* the Gulf of California and the Gulf of Mexico are important moisture sources for NAM precipitation (see Adams and Comrie 1997 and references therein). Figure 7 suggests that the degree of influence of gulf surges decreases as one progresses west to east across the NAM region.

d) Mechanism

In this section we seek a physical mechanism which connects zonal wind variability in the tropical Pacific with gulf surges over 15° latitude to the north.

As noted in previous studies (Stensrud et al. 1997; Fuller and Stensrud 2000; Douglas and Leal 2003), gulf surges are typically associated with the passage of easterly waves over Mexico several days earlier. Using time-lagged regression of meridional wind on the S AZ index, we also find strong evidence for a connection between easterly waves and S AZ precipitation. Looking at figure 8, we can trace meridional wind anomalies at lag = 0 backward in time to the Caribbean Sea (longitude < 90°W). A similar plot for SW NM does *not* show a pronounced signal (Fig 8b).

The connection between NAM precipitation and easterly waves 15° to the south suggests a mechanism whereby MJO variability can effect NAM precipitation. Previous studies have documented the important role of the MJO in modulating easterly waves in the East Pacific (Maloney and Hartmann 2001; Hartmann and Maloney 2001). During the westerly phase of the MJO, the background flow in the East Pacific encourages the amplification of waves off the coast of Mexico. The amplification of these easterly waves

off the Mexican coast makes it more likely for the waves to trigger the development of a gulf surge. Figure 9 shows the weekly mean wind anomalies (arrows) as well as the kinetic energy of the deviations from the weekly mean (transient K.E., contours) one week before S AZ precipitation. The anomalous transient kinetic energy preceding S AZ rain is in the same location where Maloney and Hartmann (2001) find the flow during the westerly MJO phase is favorable for wave growth (compare Fig. 9 with their Fig. 7). Thus it appears that the MJO affects NAM precipitation by amplifying easterly waves in the region critical for triggering the development of a gulf surge. The details of how easterly waves trigger a gulf surge are not clear (e.g. Stensrud et al. 1997).

We close this section by providing a summary of the "typical" progression of events in the eastern tropical Pacific which lead to S AZ precipitation (Fig. 10). Eight days before S AZ precipitation, the most obvious feature is the MJO zonal wind pattern at 12.5°N (Fig. 10a). In addition, we see southerlies north of Honduras (lon = 85°W, lat = 17.5°N) which are the same as the eastward propagating feature evident in figure 8a. By lag = -6 days, these southerlies have propagated eastward over the Yucatan Peninsula and additional southerlies have begun to appear on the Pacific side of the Mexican highlands. These additional southerlies are part of the cyclonic vortex spinning up on the northern, cyclonic flank of the MJO zonal wind anomalies (Fig. 10b). By lag = -4 days, the MJO zonal wind anomalies are significantly weaker than 4 days previous and the cyclonic vortex has grown and moved 2.5° northward. The growth and movement of the vortex continue at lag = -2 days so that the flow looks very much like a gulf surge at this time. Also note the northerlies north of Honduras which represent the opposite phase of the

subtropical, easterly wave at this location than at lag = -8 days. The lag = 0 plot is shown in figure 5a.

The growth of the "gulf surge vortex" evident in figure 10 is clearly not just attributable to the MJO anomalies because there is also the simultaneous development of high pressure and associated winds over the U.S. which reinforce the vortex (compare lag = -4 days to lag = -6 days). It appears that this high pressure anomaly is associated with a mid-latitude wave train propagating from the Pacific (not shown). Evidently, AZ precipitation is largest when the mid-latitude waves and easterly, subtropical waves are optimally located. The importance of both the mid-latitude and the subtropical waves in triggering gulf surges has also been suggested by Stensrud et al. (1997). Interestingly, the NW Mex. precipitation index is significantly less correlated with mid-latitude wave trains than the S AZ precipitation index (not shown).

5. Conclusions

Zonal wind anomalies in the eastern tropical Pacific associated with the MJO cause above normal precipitation in the monsoon region of North America from several days to over a week later. The MJO appears to contribute to the development of surges of moisture up the Gulf of California. Thus the time lag between the tropical zonal wind anomalies and monsoon precipitation increases as one moves northward along the gulf of California and into the southwestern U.S. A similar connection between the MJO and New Mexico precipitation is absent, presumably because New Mexico precipitation is not influenced much by gulf surges.

The mechanism linking the MJO and monsoon precipitation involves easterly waves propagating into the Pacific from the Caribbean Sea. Previous studies have already

documented the important role of easterly waves off the coast of Mexico in triggering a gulf surge (Stensrud et al. 1997; Fuller and Stensrud 2000; Douglas and Leal 2003). The westerly phase of the MJO appears to increase monsoon precipitation by amplifying easterly waves in the region critical for triggering the development of a gulf surge.

Acknowledgments

This work was supported by NOAA's CLIVAR Pan American Climate Studies (PACS) under grant GC00-358.

References

Adams, D. K. and A. C. Comrie, 1997: The North American monsoon. *Bull. Amer. Meteor. Soc.*, **78**, 2197-2213.

Charba J. P., A. W. Harrell III, and A. C. Lackner III, 1992: A monthly precipitation amount climatology derived from published atlas maps: Development of a digital database. TDL Office Note 92-7, National Weather Service, NOAA, U.S. Department of Commerce, 20 pp.

Cressman, G. P., 1959: An operational objective analysis system. *Mon. Wea. Rev.*, **87**, 367-374.

Douglas, M. W., R. A. Maddox, K. Howard and S. Reyes, 1993: The Mexican monsoon. *J. Climate*, **6**, 1665-1677.

Douglas, M. W., and J. C. Leal, 2003: Summertime surges over the Gulf of California: aspects of their climatology, mean structure, and evolution from radiosonde, NCEP reanalysis, and rainfall data. *Wea. Forecasting*, **18**, 55-74.

Fuller, R. D., and D. J. Stensrud, 2000: The relationship between tropical easterly waves and surges over the Gulf of California during the North American monsoon. *Mon. Wea. Rev.*, **128**, 2983-2989.

Glahn, H. R., T. L. Chambers, W. S. Richardson, and H. P. Perrotti, 1985: Objective map analysis for the Local AFOS MOS program. NOAA Tech. Memo. NWS TDL 75, National Weather Service, NOAA, U.S. Department of Commerce, 34 pp.

Hartmann, D. L. and E. D. Maloney, 2001: The Madden-Julian Oscillation, barotropic dynamics, and North Pacific tropical cyclone formation. Part II: Stochastic barotropic modeling. *J. Atmos. Sci.*, **58**, 2559-2570.

Higgins, R. W., W. Shi, E. Yarosh, R. Joyce, 2000: Improved United States Precipitation Quality Control System and Analysis. NCEP/Climate Prediction Center ATLAS No. 7, 40 pp.

Higgins, R. W., W. Shi, 2001: Intercomparison of the principal modes of interannual and intraseasonal variability of the North American monsoon system. *J. Climate*, **14**, 403-417.

Kalnay, E. M., Coauthors, 1996: The NCEP/NCAR 40-Year Reanalysis Project. *Bull. Amer. Meteor. Soc.*, **77**, 437-471.

Madden, R. A., and P. R. Julian, 1971: Detection of a 40-50 day oscillation in the zonal wind in the tropical Pacific. *J. Atmos. Sci.*, **28**, 702-708.

Madden, R. A., and P. R. Julian, 1994: Observations of the 40-50 day tropical oscillation -A review. *Mon. Wea. Rev.*, **122**, 814-837.

Maloney, E. D., D. L. Hartmann, 1998: Frictional moisture convergence in a composite life-cycle of the Madden-Julian oscillation. *J. Climate*, **11**, 2387-2403.

Maloney, E. D., D. L. Hartmann, 2001: The Madden-Julian oscillation, barotropic dynamics, and North Pacific tropical cyclone formation. Part I: Observations. *J. Atmos. Sci.*, **58**, 2545-2558.

Stensrud, D. J., R. L. Gall, M. K. Nordquist, 1997: Surges over the Gulf of California during the Mexican Monsoon. *Mon. Wea. Rev*., **125**, 417-437.

Figure Captions

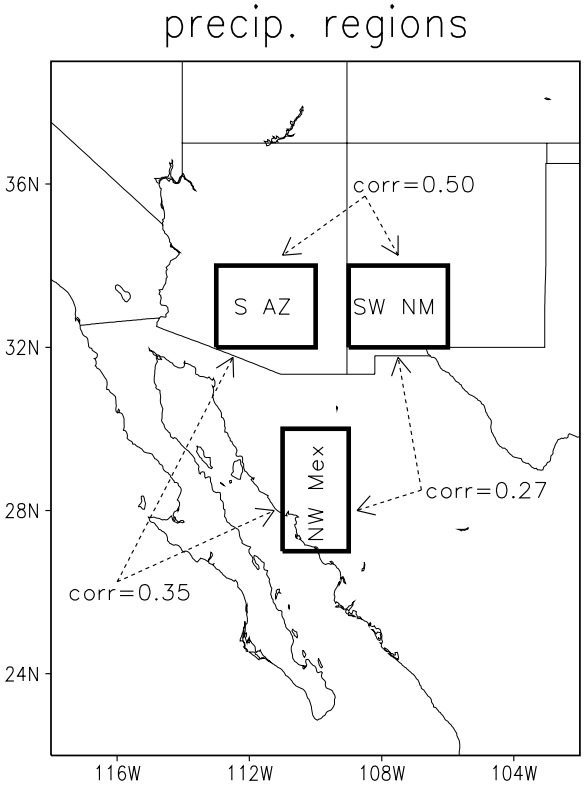

Figure 1: The three regions which define the three precipitation indices are highlighted in thick rectangles. The names of the regions are included as well as the correlation of precipitation between the regions for weekly-mean data.

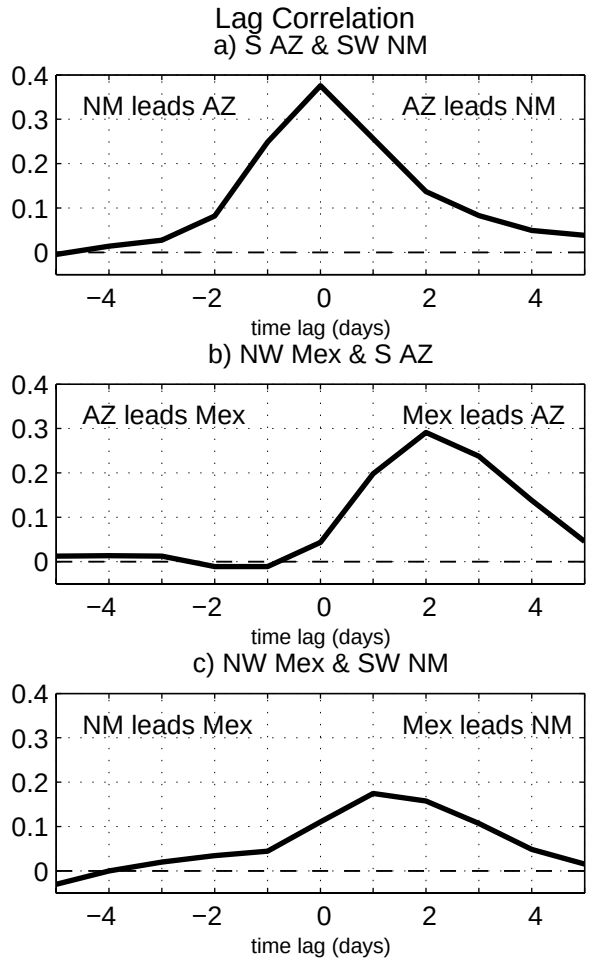

Figure 2: The lag-correlation between the between the time series of precipitation in the three regions: S AZ, SW NM and NW Mex. The calculation is done using daily data.

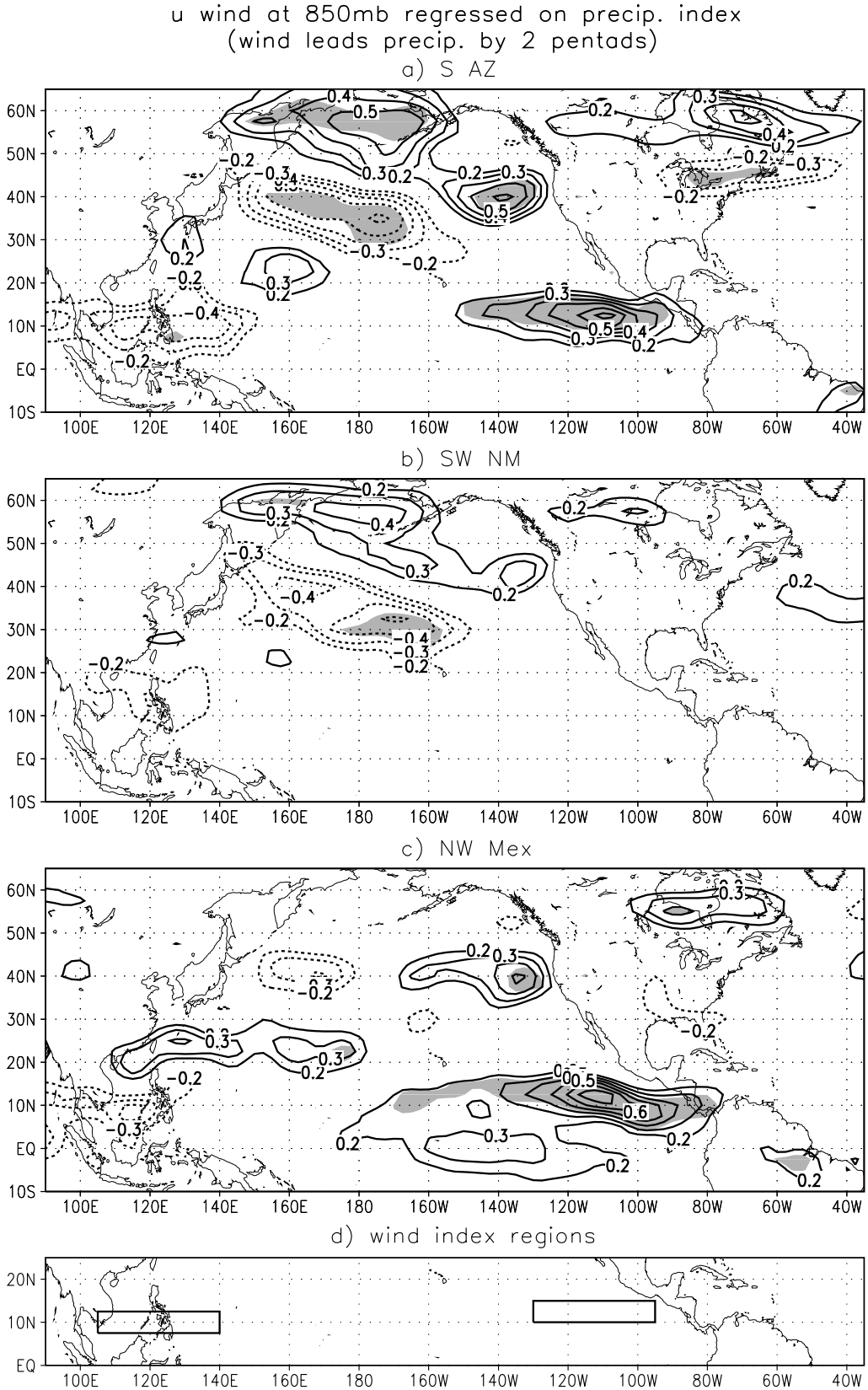

Figure 3: 850mb zonal wind anomalies regressed on each of the precipitation indices. The regression is done using pentad data with the zonal wind anomalies leading the precipitation by two pentads. The statistically significant features are shaded (95%). The units are m/s. a) S AZ. b) SW NM. c) NW Mex. d) The two rectangles highlight the regions used to define the West Pacific and East Pacific zonal wind indices.

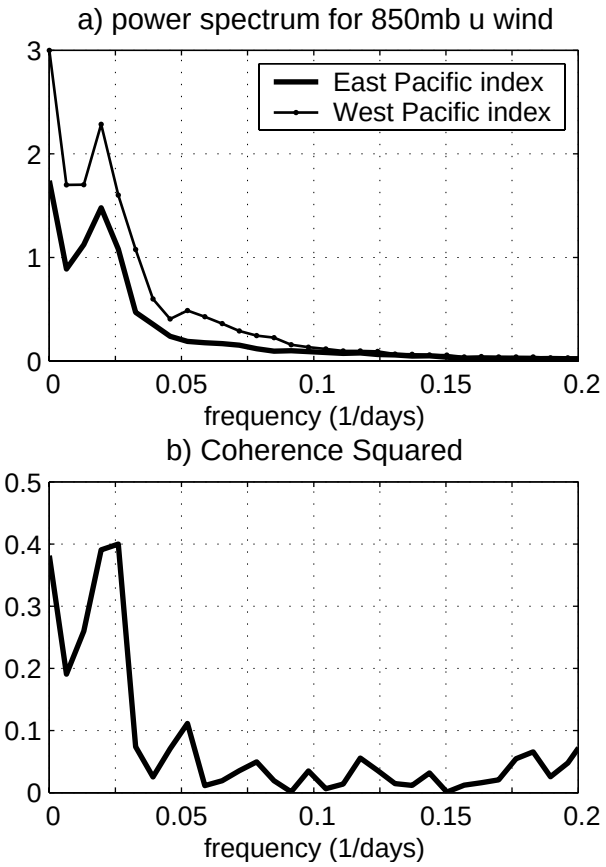

Figure 4: a) The power spectra of the 850mb zonal wind time series in the West and East Pacific. The spectra were computed using data from the entire warm season (May 1 to Sept. 30) so that low frequencies can be resolved. In addition, the seasonal-mean has not been removed so that one can compare interannual variability (frequency = 0) with intraseasonal variability. b) Coherence squared between the West and East Pacific time series.

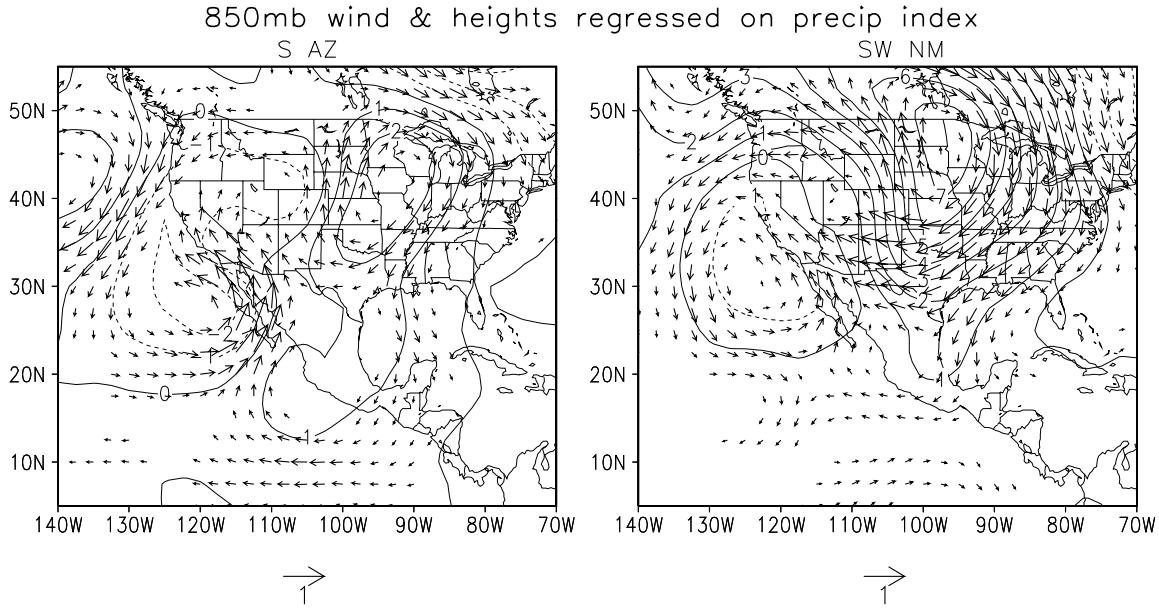

Figure 5: 850mb wind (vectors) and height (contours) anomalies regressed on the a) S AZ and b) SW NM precipitation time series. The regression is done with daily data and there is *no* time lag. The units are m/s for wind and m for the heights.

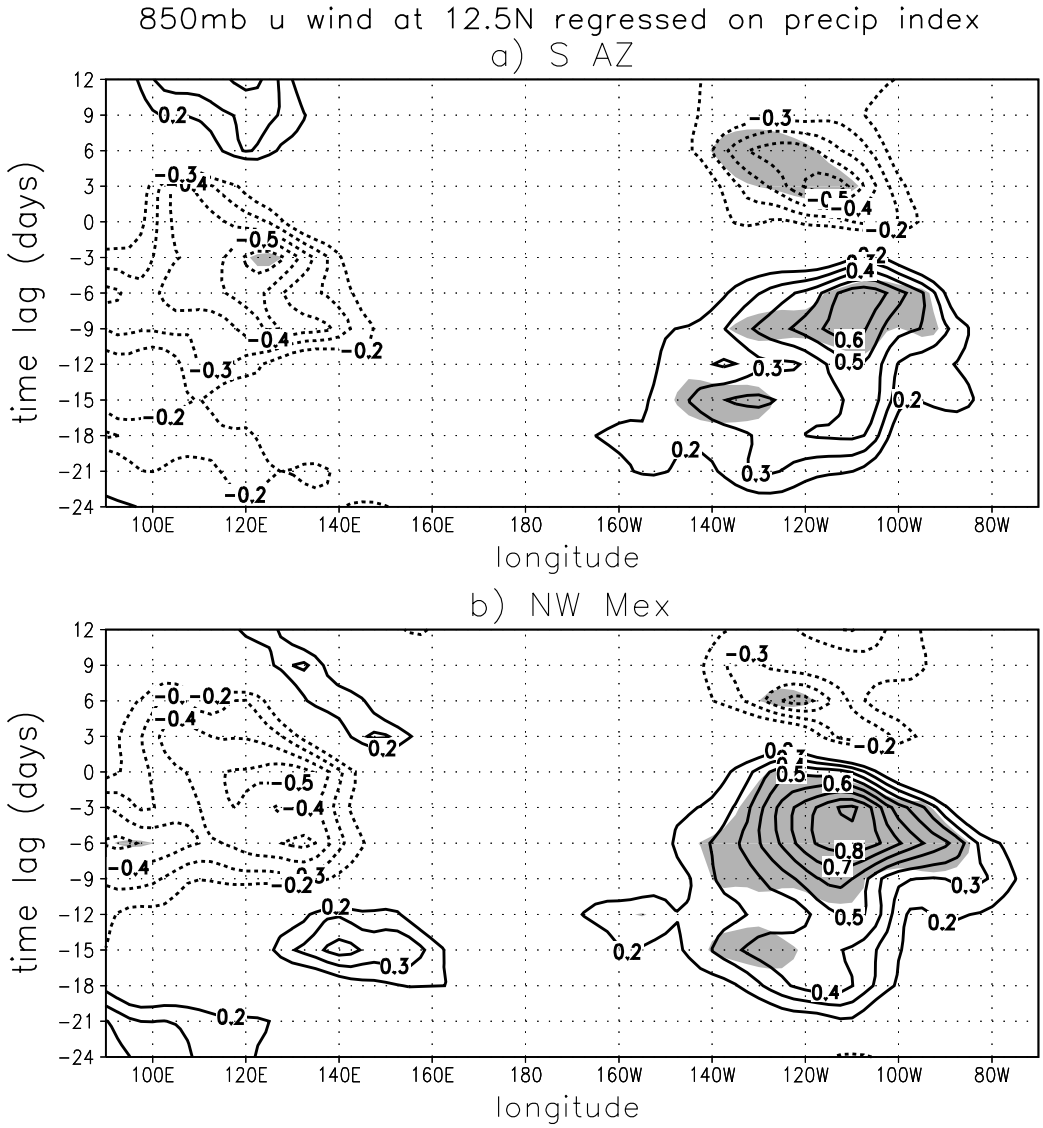

Figure 6: 850mb zonal wind anomalies along 12.5°N regressed on the a) S AZ and b) NW Mex. precipitation time series. The regression is done for a range of time lags using triad (3-day-mean) data. The statistically significant features are shaded (95%). The units are m/s.

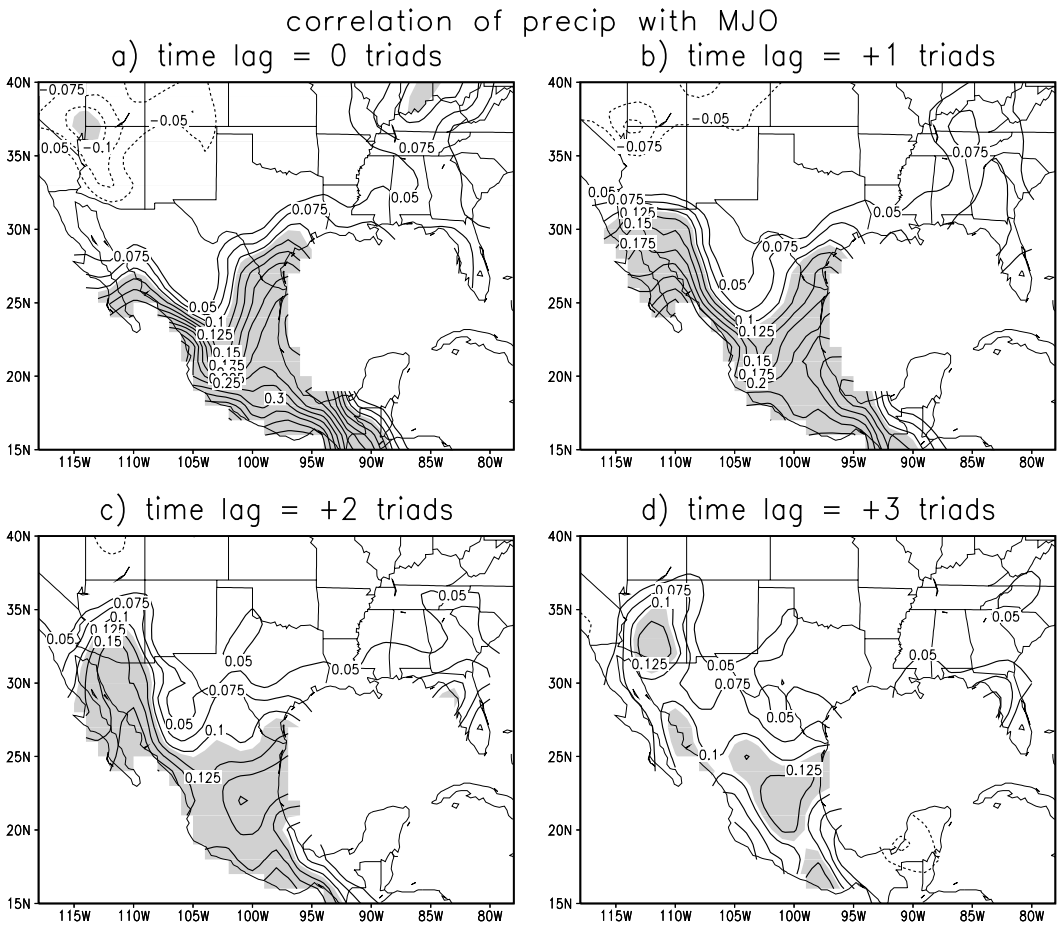

Figure 7: The correlation between the precipitation anomalies at each grid point and the East Pacific zonal wind index for a range of time lags. The correlation was computed using triad (3-day-mean) data. The statistically significant features are shaded (95%).

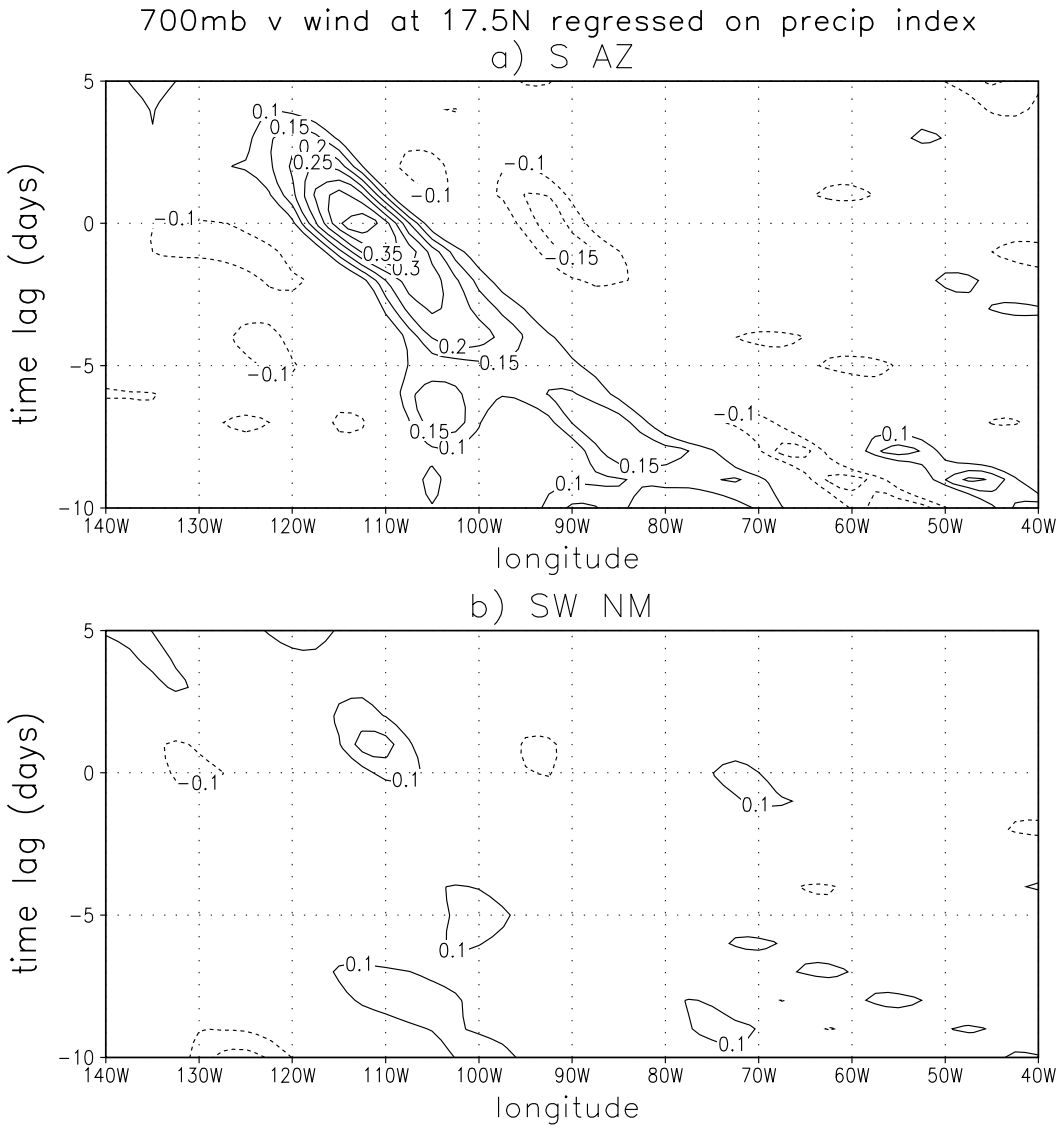

Figure 8: 700mb meridional wind anomalies along 17.5°N regressed on the a) S AZ and b) SW NM precipitation time series. The regression is done for a range of time lags using daily data. The units are m/s.

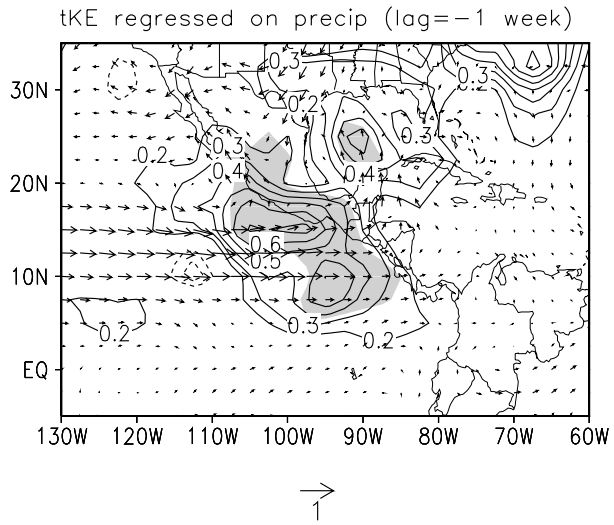

Figure 9: 850mb wind anomalies (vectors) and transient kinetic energy anomalies (contours) regressed on the S AZ precipitation time series. The regression was done using weekly mean data. The transients are defined to be the deviation from the weekly-mean. The units are m/s for wind and m^2/s^2 for transient kinetic energy.

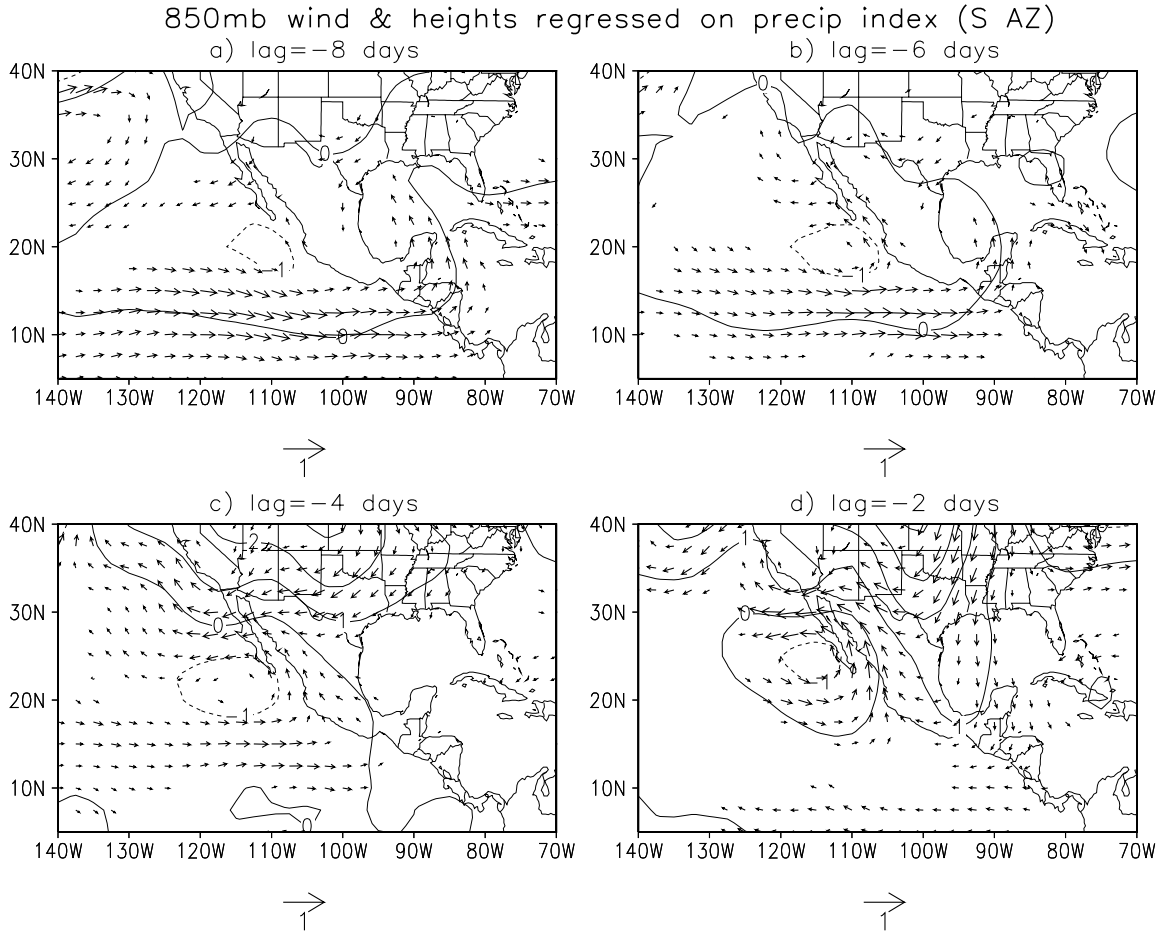

Figure 10: 850mb wind (vectors) and height (contours) anomalies regressed on the S AZ precipitation time series for different time lags. The regression is done with daily data. The units are m/s for wind and m for the heights. Note that the map scale, vector lengths and contour interval are the same as Fig. 5a which shows the corresponding plot for time lag=0 days.

Table Captions

Table 1: The starting and ending dates of the monsoon season.

	daily	triad	pentad	weekly
start of season	June 28	June 28	June 29	July 1
end of season	Sept. 1	Sept. 1	Sept. 1	Sept. 1

Table 2: Boundaries of the precipitation regions used to define the 3 precipitation indices.

	S AZ	SW NM	NW Mex.
longitude range	110°W to 113°W	106°W to 109°W	109°W to 111°W
latitude range	32°N to 34°N	32°N to 34°N	27°N to 30°N